

Security of differential phase shift QKD against explicit individual attacks

Valliamai Ramanathan and Anil Prabhakar

Department of Electrical Engineering, Indian Institute of Technology Madras, Chennai - 600036, India.

Prabha Mandayam

Department of Physics, Indian Institute of Technology Madras, Chennai 600036, India.

(Dated: March 13, 2024)

Quantum key distribution (QKD) is known to be unconditionally secure in principle, but quantifying the security of QKD protocols from a practical standpoint continues to remain an important challenge. Here, we focus on phase-based QKD protocols and characterize the security of the 3 and n -pulse Differential Phase Shift Quantum Key Distribution (DPS QKD) protocols against individual attacks. In particular, we focus on the minimum error discrimination (MED) and cloning attacks and obtain the corresponding shrinking factor by which the sifted key needs to be shrunk in order to get a secure key. We compare the secure key rates thus obtained with the known lower bounds under a general individual attack. In a departure from the theoretical lower bounds, which have no explicit attack strategies, our work provides a practical assessment of the security of phase-based protocols based on attacks with known implementations.

I. Introduction

Quantum Key Distribution (QKD) offers the promise of secure communication over public networks, ideally, with *unconditional security* [1–3]. In practice, this notion of unconditional security is compromised by device imperfections and detector efficiencies. Furthermore, different QKD implementations are susceptible to different kinds of eavesdropping attacks. Researchers consider individual attacks of intercept-resend [4], and photon number splitting (PNS) [5, 6], collective attacks [7] and general coherent attacks. We refer the reader to review articles for a comprehensive survey of the known secure key rate estimates, both in the ideal case as well as in the imperfect scenarios [8, 9].

The security of QKD relies on fundamental properties of quantum systems including monogamy of entanglement, the no-cloning principle, and the uncertainty principle [10]. Quantitatively, the security of a specific QKD implementation is characterised by its secure key rate [11, 12]. Both asymptotic and finite key security analyses have been presented for the standard QKD protocols in the literature [13–16]. The former is easier and assumes an infinite key length, which might be unrealistic, whereas the latter takes into account the finite length size of the key.

In this paper, we focus on the specific class of differential phase shift (DPS) QKD protocols [17–19]. This class of distributed phase-reference protocols is known for its simplicity and efficient key generation. DPS QKD does not require basis reconciliation as in the case of the BB84 protocol and thus every bit that is detected contributes to the key. The ease of implementation of this protocol makes it of practical interest [20, 21]. There are several variations of this protocol including round-robin DPS [22], the small-number-random DPS protocol [23], and measurement-device-independent DPS (MDI-DPS) [24].

While the DPS protocol was originally proven to be secure against the basic individual attacks such as the intercept-resend and beam splitter attacks, it was subsequently shown to be secure against more general individual attacks [25]. Unconditional security was then proved under general coherent attacks for single photon DPS QKD [26]. In proving unconditional security, the eavesdropper is

considered to be capable of entangling ancillary systems to blocks of pulses and performing operations that are dependent on previous measurement results. Specific collective attacks on weak coherent based implementation have also been studied in the past [27]. More recently, there have been formal proofs of security for the weak-coherent-state based DPS-QKD [28, 29] protocol.

In this work, we study two specific kinds of individual attacks, the minimum error discrimination (MED) attack and the cloning attack. The effects of these attacks on the secure key rate of the DPS QKD protocol are yet to be quantified. Note that the individual eavesdropping strategy, the simplest class of strategies, is still technologically very challenging to achieve today in an optimal way. The MED attack is similar to the unambiguous state discrimination (USD) attack, except that the eavesdropper makes some errors in identification. Recall that unambiguous state discrimination (USD) is only possible for states that are linearly independent [30]. Since the ideal (single-photon) $n \geq 3$ -pulse DPS states are linearly dependent, the corresponding protocols are naturally secure against a USD-type attack. In past work, an intercept and resend attack has been considered wherein the eavesdropper (Eve) uses the same setup as the receiver (Bob) [18]. In the current work, we consider the scenario where Eve does minimum error discrimination (MED) of the states after intercepting them. This constitutes the first part of the study. MED is based on a detection theory [31] and has been studied in the past in the context of other phase-based protocols such as the coherent one-way protocol [32].

The second part of our work analyzes the security of the DPS QKD protocol against a cloning attack. The cloning attack has been previously studied for QKD protocols such as BB84 and the six-state protocol [33–35], and has also been used as a counterfeiting procedure for quantum money [36]. The problem of finding the *optimal* quantum cloner is a convex optimization problem and can be formulated as a semidefinite program. In our work, we assume that the eavesdropper uses a symmetric quantum cloning machine that maximizes the cloning fidelity for the 3-pulse DPS QKD protocol. Both the MED measurement and the cloning machine maps are optimized to achieve the max-

imum information gain for an eavesdropper by recasting them as semidefinite programs.

The rest of the paper is organized as follows. In Sec. II we briefly review the DPS QKD protocol. Sec. III describes the MED of quantum states and formulates the MED attack for the 3-pulse and n -pulse DPS protocols. In Sec. IV the description of a cloning attack against 3-pulse DPS is provided, along with the error rates introduced. In Sec. V we deviate a little from the map-based optimal cloning and look at how a unitary transformation based cloning utilizing only one cloning ancillary system performs as compared to the optimal map-based cloning.

II. Preliminaries

We begin with a brief review of the n -pulse DPS QKD protocol [17, 18], schematically shown for the $n = 3$ case in Fig. 1. We note that this schematic can be easily extended to n pulses by simply introducing more delay lines at the source, or using an equivalent time-bin phase modulation [20]. The sender (Alice) prepares a photon in an equal superposition of $n \geq 3$ pulses and encodes her bit values $\{0, 1\}$ via the relative phases $\{0, \pi\}$. The states sent by Alice in the $n = 3$ case can be written as,

$$|\psi\rangle_{\pm, \pm} = \frac{1}{\sqrt{3}}(|1\rangle_1|0\rangle_2|0\rangle_3 \pm |0\rangle_1|1\rangle_2|0\rangle_3 \pm |0\rangle_1|0\rangle_2|1\rangle_3). \quad (1)$$

Here $|i\rangle_j$ refers to i photons in the j^{th} path. Or equivalently, a specific DPS state can be written as,

$$|\psi\rangle_{+,+} = \frac{1}{\sqrt{3}} [a_1^\dagger + a_2^\dagger + a_3^\dagger] |0\rangle \quad (2)$$

where a_i^\dagger refers to the creation operator at the i^{th} path. The set of states sent by Alice in the 3-pulse DPS protocol belongs to a three-dimensional Hilbert space spanned by the basis states,

$$\begin{aligned} |1\rangle_1|0\rangle_2|0\rangle_3 &\triangleq |1\rangle \\ |0\rangle_1|1\rangle_2|0\rangle_3 &\triangleq |2\rangle \\ |0\rangle_1|0\rangle_2|1\rangle_3 &\triangleq |3\rangle. \end{aligned}$$

Thus, the signal states sent by Alice can be written in vector form as,

$$\begin{aligned} |\psi\rangle_{+,+} &= (1/\sqrt{3})[1, 1, 1]^T, \\ |\psi\rangle_{+,-} &= (1/\sqrt{3})[1, -1, 1]^T, \\ |\psi\rangle_{-,+} &= (1/\sqrt{3})[1, 1, -1]^T, \\ |\psi\rangle_{-,-} &= (1/\sqrt{3})[1, -1, -1]^T. \end{aligned}$$

The receiver (Bob) uses an unbalanced Mach Zehnder interferometer (MZI) for decoding, detects the relative phase between the pulses, and hence obtains the bit value sent by Alice. On Bob's side, the detection at the first and the last time slots are random and are not used in generating the shared key. Detection in any of the other $n - 1$ time slots gives the key bits, wherein the bit-value is assigned based on which detector (constructive or destructive) clicks. In

the ideal case, when a single photon is sent in a superposition of n pulses, the sifted key rate is obtained as,

$$R_{\text{sifted}} = \frac{n-1}{n}. \quad (3)$$

The security of this DPS protocol is based on the fact that the states in Eq. (1) are non-orthogonal and hence cannot be distinguished perfectly.

A. Secure key rate

The security of any QKD implementation can be quantified via its secure key rate. Assuming that the eavesdropper is restricted to only individual attacks, the secure key rate can be calculated for the DPS QKD protocol as [21],

$$R_{\text{sk}} = R_{\text{sifted}} [\tau - f(e_b) [h(e_b)]]. \quad (4)$$

Here, $R_{\text{sifted}} = sp_{\text{click}}$, where $s = 2/3$ is the sifting parameter, p_{click} is the probability of Bob's detection taking into account detector efficiencies, e_b is the bit error rate, and $f(e_b)$ characterizes the performance of the error correction algorithm. The parameter τ represents the shrinking factor due to privacy amplification and is calculated from the average collision probability, and, $h(e_b)$ is the binary Shannon entropy [21], defined as,

$$h(e_b) = -[e_b \log_2 e_b + (1 - e_b) \log_2 (1 - e_b)] \quad (5)$$

The key rate given above is in the asymptotic limit. The two terms in the expression, τ and $f(e_b)[h(e_b)]$ relate to privacy amplification and error correction respectively. Based on Shannon's noiseless coding theorem, the minimum number of bits that must be exchanged publicly for error correction equals the binary entropy of the bit error rate e_b . The bit error rate e_b has contributions from both the signal and dark counts. The error in the signal states can be due to imperfect state preparation too. The dark counts are uncorrelated to Alice's key and thus have a 50 percent chance of being wrong. The bit error rate is thus

$$e_b = \frac{0.5p_{\text{dark}} + B \cdot p_{\text{signal}}}{p_{\text{click}}}, \quad (6)$$

where B is the baseline system error rate quantifying the imperfect state preparation, p_{dark} is dark count probability, p_{signal} is the probability of getting a click due to a photon given channel loss, distance and detector efficiency, and $p_{\text{click}} = p_{\text{dark}} + p_{\text{signal}}$. All the system's errors are usually given as an advantage to Eve and thus the role of privacy amplification is to deduce the shrinking factor τ by which the key rate has to be shrunk to bound the information leaked to Eve. The shrinking factor τ is a function of the average collision probability p_c ,

$$\tau = -\log_2 p_c. \quad (7)$$

The average collision probability quantifies Eve's mutual information with Alice and Bob and can be evaluated in terms of the individual collision probability of each bit, denoted as p_{c0} . In fact, for individual attacks, the overall collision probability is simply the product of the individual collision probabilities. Specifically, p_{c0} is set to 1 for

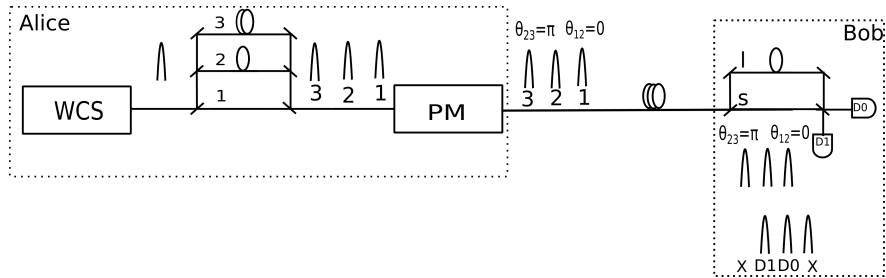


FIG. 1: The 3-pulse DPS QKD protocol. PM - Phase Modulator, θ_{12} and θ_{23} are the phase introduced between the pulses by the phase modulator. $\theta_{12}, \theta_{23} \in \{0, \pi\}$. D0 and D1 are single photon detectors. Detection in the second and the third time slot gives θ_{12} and θ_{23} respectively.

the bits that are detected correctly by Eve and 1/2 for the bits unknown to Eve [21]. In general, the average collision probability is given as [25]

$$p_{\text{co}} = \sum_{x,z} p^2(X_i = x | Z_i = z) p(Z_i = z), \quad (8)$$

where X and Z are Alice's and Eve's key bit string and Eve's information respectively. In [25], the most general individual attack is considered and a bound on the collision probability for each bit is found to be

$$p_{\text{co}} \leq 1 - e_b^2 - (1 - 6e_b)^2/2.$$

Using this value in Eq. (4) gives a lower bound on the secure key rate obtained against individual attacks for DPS QKD [25],

$$R_{\text{ind}} = -p_{\text{click}} [-\log_2 p_{\text{co}} + f(e_b)h(e_b)]. \quad (9)$$

Here the first term, $-\log_2 p_{\text{co}}$ is the shrinking factor (τ_{low}) The unconditional security proof in [26] gives a bound on the phase error rate by assuming a general coherent attack and lower bound on the secure key rate is given as

$$R_{\text{sk}} \geq R_{\text{sifted}} \left[1 - h(e_b) - h((3 + \sqrt{5})e_b) \right]. \quad (10)$$

This expression holds for n -pulse DPS with R_{sifted} depending on n . In our work, we consider an adversary who will apply an individual and identical attack based on MED and cloning. There is no assumption that Eve holds any information intercepted in quantum memory. We now proceed to study the different individual attacks and evaluate the corresponding secure key rates.

III. Minimum error discrimination attack

In the minimum error discrimination (MED) attack, the eavesdropper (Eve) aims to identify the optimal quantum measurements required to discriminate the signals transferred through a channel during QKD. The minimum error condition is enforced by maximizing the success probability of the state discrimination. Minimum error discrimination can be described mathematically as follows.

Suppose Alice prepares a set of N states $\{|\psi_1\rangle, |\psi_2\rangle, \dots, |\psi_N\rangle\}$ which are non-orthogonal and

linearly dependent. She chooses the state $|\psi_i\rangle$ with probability $p(i)$ and sends it to Bob. Eve uses a positive operator valued measure (POVM) comprising a set of n positive operators denoted as $\{P_1, \dots, P_N\}$ such that outcome i associated with measurement operator P_i corresponds to state $|\psi_i\rangle$. Let $\{\rho_i = |\psi_i\rangle\langle\psi_i|\}$ denote the density operators corresponding to Alice's signal states. Then, the average success probability corresponding to Eve's POVM is, $\sum_i p(i)\text{Tr}[P_i\rho_i]$. The problem of minimum error discrimination is to maximize this success probability and following [37], this can be recast as a semidefinite program (SDP), as described below.

$$\begin{aligned} & \text{maximize} && \sum_{i=1}^N \langle \sigma_i, P_i \rangle \\ & \text{subject to} && P_i \geq 0 \\ & && \sum_{i=1}^N P_i = I \end{aligned} \quad (11)$$

where $\sigma_i = p(i)\rho_i$ and $\langle \sigma_i, P_i \rangle = \text{Tr}[\sigma_i P_i]$ denotes the Hilbert-Schmidt inner product between the positive operators σ_i and P_i . We can therefore use an SDP solver to find the optimal success probabilities and the corresponding POVM for minimum error discrimination of a set of quantum states.

A. MED of the ideal 3-pulse DPS QKD states

The ideal single-photon 3-pulse DPS QKD protocol shown in Fig.1 encodes the logical bits as relative phases. The states sent by Alice can be written as in Eq. (1). We assume that Alice sends the four states with equal probability, that is, $\frac{1}{4}$. Thus to do a minimum error discrimination of these four states, Eve tries to identify the optimal POVM with four elements $\{P_1, P_2, P_3, P_4\}$, where each POVM element correctly identifies one state. The SDP corresponding to minimum error discrimination of the 3-pulse DPS states is therefore written as,

$$\begin{aligned} & \text{maximize:} && \sum_i \frac{1}{4} \langle \rho_i, P_i \rangle \\ & \text{subject to:} && \sum_i P_i = I \\ & && P_i \geq 0 \end{aligned} \quad (12)$$

where, ρ_i is the density matrix corresponding to the DPS states.

We solve this SDP using the cvx solver [38, 39] and summarize the detection probabilities in Table I. We see that each state has a 75% chance of being correctly identified

TABLE I: Optimal measurement probabilities for 3-pulse DPS states. $|\psi\rangle$'s represent the DPS state and $\{P_i\}$ the POVM elements

	P_1	P_2	P_3	P_4
$ \psi\rangle_{+,+}$	0.75	0.083	0.083	0.083
$ \psi\rangle_{+,-}$	0.083	0.75	0.083	0.083
$ \psi\rangle_{-,+}$	0.083	0.083	0.75	0.083
$ \psi\rangle_{-,-}$	0.083	0.083	0.083	0.75

by Eve. The positive operators that constitute this optimal POVM are as given below.

$$P_1 = \begin{bmatrix} 0.25 & 0.25 & 0.25 \\ 0.25 & 0.25 & 0.25 \\ 0.25 & 0.25 & 0.25 \end{bmatrix} \quad P_2 = \begin{bmatrix} 0.25 & -0.25 & 0.25 \\ -0.25 & 0.25 & -0.25 \\ 0.25 & -0.25 & 0.25 \end{bmatrix}$$

$$P_3 = \begin{bmatrix} 0.25 & 0.25 & -0.25 \\ 0.25 & 0.25 & -0.25 \\ -0.25 & -0.25 & 0.25 \end{bmatrix} \quad P_4 = \begin{bmatrix} 0.25 & -0.25 & -0.25 \\ -0.25 & 0.25 & 0.25 \\ -0.25 & 0.25 & 0.25 \end{bmatrix}$$

B. Intercept and resend attack with MED

The optimal MED for the 3-pulse DPS states shows that Eve has a 75% probability of correctly identifying a given state. We had previously considered an intercept and resend attack where Eve uses the same apparatus as Bob, and introduced errors in 33% of the intercepted bits [18]. But in an intercept attack using MED, Eve introduces only a 25% error. We now compare the key rate in the presence of these two attacks.

To find the secure key rate in the presence of an MED attack, one has to find the collision probability and the corresponding shrinking factor. The collision probability is defined as in Eq. (8), with $P(X|Z)$ being the probability of guessing Alice's string given Eve's information Z . In the case of an MED attack, Eve's information corresponds to which of the POVMs clicked. Therefore $Z \in \{P_1, P_2, P_3, P_4\}$. Alice's bit value is either 0 or 1 that is $X \in \{0, 1\}$, which can in turn be detected from the phase difference between the first and the second time bin or the second and third, both the cases being equally probable. Now,

$$\begin{aligned} p_{co} &= \sum_{x,z} P^2(X=x|Z=z)P(Z=z) \\ &= \sum_{i=1}^4 P^2(X=0|Z=P_i)P(P_i) + \\ &\quad P^2(X=1|Z=P_i)P(P_i) \\ &= 1/2 \left[\sum_{i=1}^4 P^2(X=0_1|Z=P_i)P(P_i) + \right. \\ &\quad \left. P^2(X=1_1|Z=P_i)P(P_i) \right] \\ &\quad + 1/2 \left[\sum_{i=1}^4 P^2(X=0_2|Z=P_i)P(P_i) + \right. \\ &\quad \left. P^2(X=1_2|Z=P_i)P(P_i) \right] \end{aligned} \quad (13)$$

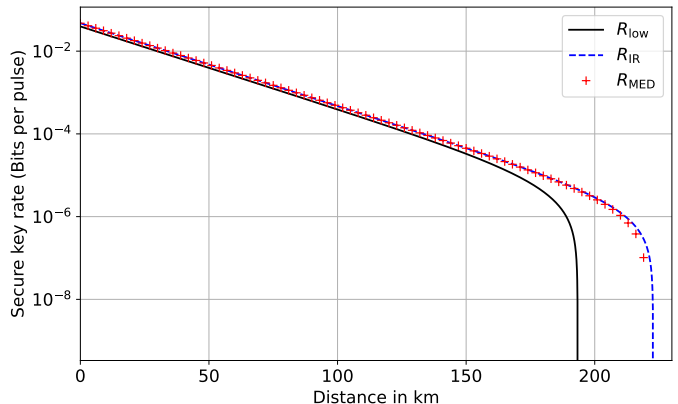


FIG. 2: Secure key rate vs distance plot for the single-photon 3-pulse DPS protocol in the presence of intercept and resend attack (R_{IR}) and minimum error discrimination attack (R_{MED}). (R_{low}) denotes the theoretical lower bound on the secure key rate [25].

The final step is to account for the fact that the bit detected can correspond to either the first phase difference or the second. The probabilities required to calculate eq. (13) are given in Table I, and the average collision probability is found to be 0.72. Now, let the probability of correct detection by Eve be denoted as p_{corr} , and the fraction of bits intercepted by Eve as n_{int}^{Eve} . To maintain the error rate at Bob's side, the fraction of bits Eve intercepts is,

$$(1 - p_{corr})n_{int}^{Eve} = e_b. \quad (14)$$

We found from the SDP that $p_{corr} = 0.75$ for the minimum error discrimination of the 3-pulse DPS states. This indicates that the fraction of bits that can be intercepted by Eve is $4e_b$. Out of these $4e_b$ pulses intercepted only two-thirds of $4e_b$ are detected by Bob in either the second or in the third time bin. Thus for a fraction of $((2/3) \cdot 4e_b)$ pulses the collision probability is 0.72 while for the remaining $(1 - (2/3) \cdot 4e_b)$ fraction of pulses the collision probability is half since they are unknown to Eve. The key rate in the presence of MED is thus given as,

$$\begin{aligned} R_{MED} &= -\frac{2}{3}p_{click} \left[-\left(\frac{2}{3} \cdot 4e_b\right) \log_2 0.72 \right. \\ &\quad \left. + \left(1 - \left(\frac{2}{3}\right) 4e_b\right) + f(e_b)h(e_b) \right] \end{aligned} \quad (15)$$

The key rate is calculated for the following implementation parameters: Channel loss of 0.2 dB/km, dark count probability of 10^{-6} , detector efficiency of 10%, and $f(e_b) = 1.16$. The key rate plots generally given on a semi-log scale does not capture the difference (Fig.2) between the lower bound and the attacks since the rates are of the same order for different attacks. We plot in Fig. 3 the shrinking factor,

$$\tau_{MED} = -\left(\frac{2}{3} \cdot 4e_b\right) \log_2 0.72 + \left(1 - \left(\frac{2}{3}\right) 4e_b\right), \quad (16)$$

and compare it with the shrinking factor corresponding to the lower bound and IR attack.

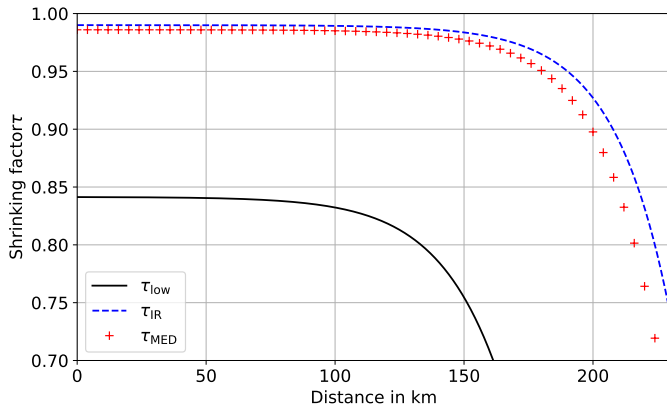


FIG. 3: Shrinking factor at different channel lengths corresponding to the lower bound (τ_{low}), IR attack (τ_{IR}) and MED attack (τ_{MED}). A channel loss of 0.2dB/Km and a detector efficiency of 10% is used in Eq. 6 to find the bit error rate and subsequently the shrinking factor.

In the 4-pulse case, Eve has to discriminate between 8 different states, and send the correct one to Bob. A POVM of 8 elements has to be set up, and the probability of the right identification maximized. This SDP problem gives out that each state is correctly identified with a probability of 0.5. Thus, in the 4-pulse case, the minimum error attack is not a strong attack. Similarly, in the 5-pulse case, the number of states goes to 16 and the probability of right identification drops further down. Hence we conclude that an MED attack using this formulation is not powerful in the case of $n > 3$ pulses. We also note that the structure of the POVM elements in the 4-pulse and the 5-pulse case looks similar to the 3-pulse case because of the symmetry in the DPS states.

Going beyond the ideal, single-photon protocol, we may ask a similar question about Eve's optimal discrimination strategy for 3-pulse DPS protocol using weak coherent states (WCS). The states sent by Alice in a WCS-based DPS protocol are of the form,

$$|\psi\rangle_{\pm,\pm} = |\alpha\rangle_k \otimes |\pm\alpha\rangle_{k+1} \otimes |\pm\alpha\rangle_{k+2},$$

where $|\alpha|^2$ is the mean photon number of the WCS source. These states being linearly independent allow for an unambiguous state discrimination (USD) attack. The secure key rate for a WCS 3-pulse DPS protocol subject to a USD attack is discussed in Appendix D.

IV. Cloning attack

We now allow the eavesdropper to have a Quantum Cloning Machine (QCM), and she tries to clone the single-photon state sent to Bob. Since the theory of quantum mechanics does not allow for perfect cloning [40], the cloned state is not a perfect copy and the initial state is disturbed in some manner. In this section, we find the bit error rate due to such imperfect cloning.

A. Cloning as an SDP problem

First we consider a cloning attack described by a quantum channel Φ , which takes a state $\rho = |\psi\rangle\langle\psi| \in \mathcal{D}(\mathcal{X})$ to the state $\Phi(\rho) \in \mathcal{D}(\mathcal{Y} \otimes \mathcal{Z})$. Here, \mathcal{D} refers to the set of density matrices on the corresponding Hilbert spaces; \mathcal{X} , \mathcal{Y} , \mathcal{Z} correspond to the senders (Alice) Hilbert space and the two receivers (Bob and Eve) respectively. The channel Φ must correspond to a completely positive and trace-preserving linear mapping of the form $\Phi : \mathcal{D}(\mathcal{X}) \rightarrow \mathcal{D}(\mathcal{Y} \otimes \mathcal{Z})$. Suppose the state sent is indexed i , a good measure that can quantify the extent of cloning is given by the fidelity, $\langle\psi_i \otimes \psi_i | \Phi(|\psi_i\rangle\langle\psi_i|) |\psi_i \otimes \psi_i\rangle$ [36]. Averaging over the possible choices of i , we get the average fidelity function corresponding to the cloning map Φ as,

$$\sum_{i=1}^N p(i) \langle\psi_i \otimes \psi_i | \Phi(|\psi_i\rangle\langle\psi_i|) |\psi_i \otimes \psi_i\rangle. \quad (17)$$

The optimal cloning strategy can then be obtained by maximizing this fidelity function over all valid channels $\Phi : \mathcal{D}(\mathcal{X}) \rightarrow \mathcal{D}(\mathcal{Y} \otimes \mathcal{Z})$. This optimization problem can again be represented by a semidefinite program [36, 41].

The formulation makes use of the Choi-Jamiołkowski representation $J(\Phi) \equiv X$ of a given channel Φ . The SDP is given as [36]

$$\begin{aligned} & \text{maximize} && \langle Q, X \rangle \\ & \text{subject to} && \text{Tr}_{\mathcal{Y} \otimes \mathcal{Z}}(X) = I_{\mathcal{X}} \\ & && X \in \text{Pos}(\mathcal{Y} \otimes \mathcal{X} \otimes \mathcal{Z}) \end{aligned} \quad (18)$$

where

$$Q = \sum_{i=1}^N p(i) |\psi_i \otimes \psi_i \otimes \bar{\psi}_i\rangle \langle\psi_i \otimes \psi_i \otimes \bar{\psi}_i|$$

Here, $\bar{\psi}$ refers to taking complex conjugation with respect to the standard basis.

B. Optimal Cloning Attack and Bit Error Rate for 3-pulse DPS states

We solve the SDP formulated in Eq. (18) for the specific case of the 3-pulse DPS states given in Eq. (1). The optimal value for the average fidelity function defined in Eq. (17) is evaluated to be 0.78. The fidelity between the original state sent by Alice and the two cloned states is 0.81 for all the states $|\psi\rangle_{\pm,\pm}$ in Alice's ensemble. Using the cvx solver, we also obtain the map Φ acting on Alice's states, from the Choi matrix. The details of the Choi matrix obtained and the details of the corresponding map are discussed in Appendix A. Interestingly, the map on Alice's states corresponding to the optimal cloner turns out to be a qutrit depolarizing map.

The bit error rate at Bob's side due to the application of the optimal cloning machine can be found using the probability of detecting in the constructive (destructive) port when the destructive (constructive) port is supposed to click. Here, we estimate the bit error rate for the optimal

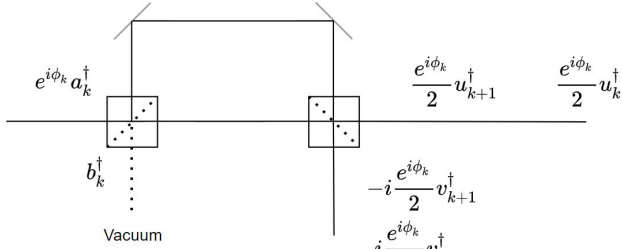


FIG. 4: Input-output relation of Bob's asymmetric MZI. a_k^\dagger , b_k^\dagger represents the creation operator at the input ports at k time and u_k^\dagger , v_k^\dagger the creation operators at the output port.

cloning attack as follows. We first note that the state received by Bob after the cloning attack is a mixed state. We write down the density matrix corresponding to this mixed state as a convex combination in an appropriate basis and calculate the probability of a wrong detection.

Consider the density matrix $\rho_{+,+}$ corresponding to Alice's input state $|\psi\rangle_{+,+}$, of the form,

$$\rho_{+,+} = \frac{1}{3} \begin{pmatrix} 1 & 1 & 1 \\ 1 & 1 & 1 \\ 1 & 1 & 1 \end{pmatrix}. \quad (19)$$

After the action of the QCM, the reduced density matrix available to Bob and Eve is

$$\tilde{\rho}_{+,+} = \begin{pmatrix} \frac{1}{3} & 0.23 & 0.23 \\ 0.23 & \frac{1}{3} & 0.23 \\ 0.23 & 0.23 & \frac{1}{3} \end{pmatrix}. \quad (20)$$

An error occurs in Bob's detector if there is a detection in the wrong port. Recall that the detector at Bob's side is an asymmetric MZI with the input-output relation shown in Fig. 4. The original state $|\psi\rangle_{+,+}$ sent by Alice in the k^{th} slot can be written in terms of the photon creation operators, as,

$$|\psi\rangle_{+,+} = \frac{1}{\sqrt{3}} \left[a_{k+2}^\dagger + a_{k+1}^\dagger + a_k^\dagger \right] |0\rangle. \quad (21)$$

Here, as before, a_k^\dagger denotes the photon creation operator at the k^{th} time slot. After $|\psi\rangle_{+,+}$ goes through the MZI, the output state is,

$$\frac{1}{\sqrt{3}} \left[\frac{u_k^\dagger}{2} + \frac{iv_k^\dagger}{2} + u_{k+1}^\dagger + u_{k+2}^\dagger + \frac{u_{k+3}^\dagger}{2} - \frac{iv_{k+3}^\dagger}{2} \right] |0\rangle. \quad (22)$$

Thus, in the ideal case, only the constructive port clicks at the $(k+1)$ and $(k+2)^{\text{th}}$ time slots.

Now let us look at what happens when the cloned state $\tilde{\rho}_{+,+}$ is received by Bob's asymmetric MZI. To calculate the probabilities of detection at different ports and time instances, we diagonalise $\tilde{\rho}_{+,+}$ and apply the MZI transformation on its eigenstates. The orthonormal basis that

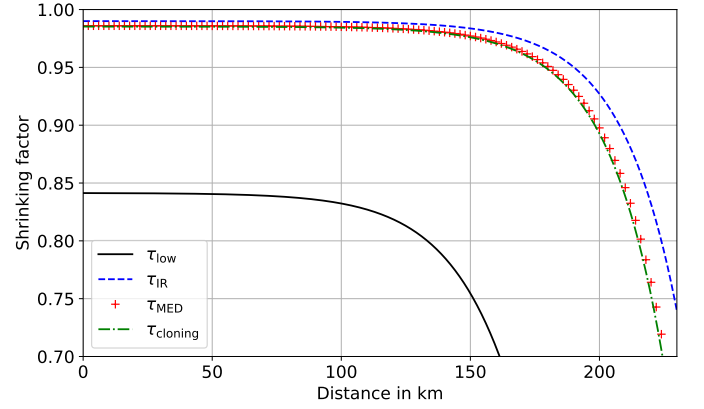


FIG. 5: Shrinking factor corresponding to the lower bound (τ_{low}), IR attack (τ_{IR}), MED attack (τ_{MED}) and cloning attack (τ_{cloning}) at different channel lengths. A channel loss of 0.2dB/Km and a detector efficiency of 10% is used in Eq. 6 to find the bit error rate.

diagonalizes the cloned state $\tilde{\rho}_{+,+}$ is

$$\begin{aligned} |e_1\rangle &= \frac{1}{\sqrt{3}} [|1\rangle + |2\rangle + |3\rangle] \\ |e_2\rangle &= \frac{1}{\sqrt{6}} [|1\rangle + |2\rangle - 2|3\rangle] \\ |e_3\rangle &= \frac{1}{\sqrt{2}} [|1\rangle - |2\rangle]. \end{aligned} \quad (23)$$

The spectral decomposition of $\tilde{\rho}_{+,+}$ can be written as,

$$\tilde{\rho}_{+,+} = 0.81|e_1\rangle\langle e_1| + 0.095|e_2\rangle\langle e_2| + 0.095|e_3\rangle\langle e_3|. \quad (24)$$

The second and third terms in Eq. (24) cause a detection in the destructive port. This erroneous click is observed due to $|e_2\rangle$ at the $(k+2)^{\text{th}}$ slot and $|e_3\rangle$ in both slots $(k+1)$ and $(k+2)$. After passing the cloned state through the MZI at Bob's side, the probability of error (in this case - the probability of clicking in the destructive port in the second and third-time bin) can be calculated as,

$$\text{BER} = 0.095 \left(\frac{3}{8} \right) + 0.095 = 0.13. \quad (25)$$

Repeating the analysis for all four DPS states, we find that the probability of wrong detection corresponding to each of the cloned states is 0.13. Once again, like in the case of the MED attack, an eavesdropper will try to clone only a number $n_{\text{int}}^{\text{Eve}}$ of states such that the error introduced due to eavesdropping matches the error introduced due to the channel.

$$p_{\text{error}} \cdot n_{\text{int}}^{\text{Eve}} = e_b$$

If the error rate in the system from signal and dark counts is e_b , for an error probability of 13% Eve can intercept $7.69e_b$ fraction of bits and remain undetected.

C. Collision probability and key rate with cloning attack

To quantify the maximum information available to an adversary, we let Eve do a minimum error discrimination of

the states reaching her after the cloning machine. We note here that since the cloning map acts like a depolarizing channel on Alice's state, the optimized POVMs are the same as that found for the pure DPS states. Since the states reaching Eve and Bob are mixed, the MED success probability is relatively less than in the case where Eve does a MED directly on the states sent by Alice. Nevertheless, this strategy does marginally better since the error introduced at Bob due to cloning is less than the direct MED, thus allowing for more bits to be attacked. Denoting the POVM elements for MED of the cloned state as CP_i , the SDP results for the right identification are as given in table II. The collision probability is found for these POVM as in the case of the MED attack and is found to be 0.61. The corresponding secure key rate is given as

$$R_{\text{Cloning}} = -\frac{2}{3}p_{\text{click}} \left[-\left(\frac{2}{3}7.69e_b\right) \log_2 0.61 + \left(1 - \left(\frac{2}{3}\right)7.69e_b\right) + f(e_b) \cdot h(e_b) \right]. \quad (26)$$

TABLE II: Measurement probabilities for the 3-pulse DPS states after the application of the optimal cloning map

	CP ₁	CP ₂	CP ₃	CP ₄
$\psi_{+,+}$	0.607	0.131	0.131	0.131
$\psi_{+,-}$	0.131	0.607	0.131	0.131
$\psi_{-,+}$	0.131	0.131	0.607	0.131
$\psi_{-,-}$	0.131	0.131	0.131	0.607

We plot in Fig. 5, the shrinking factor for the attacks discussed so far.

V. A QCM based on unitary transformation

In this section we look at a simpler quantum cloning machine based on a unitary transformation [42] on a tripartite system $\mathcal{H}_A \otimes \mathcal{H}_B \otimes \mathcal{H}_C$, where \mathcal{H}_A denotes the Hilbert space of the state to be cloned, \mathcal{H}_B denotes the ancillary system into which the copy is made and \mathcal{H}_C denotes the Hilbert space associated with the cloner. Suppose \mathcal{H}_A and \mathcal{H}_B are Hilbert spaces of dimension d . Let $\mathcal{B} \equiv \{|e_i\rangle_A, 1 \leq i \leq d\}$ denote a fixed orthonormal basis in \mathcal{H}_A . The symmetric QCM is then defined via the linear transformation [42, 43],

$$|e_i\rangle_A |0\rangle_B |X\rangle_C \rightarrow p|e_i\rangle_A |e_i\rangle_B |X_i\rangle_C + q \sum_{j \neq i} (|e_i\rangle_A |e_j\rangle_B + |e_j\rangle_A |e_i\rangle_B) |X_j\rangle_C. \quad (27)$$

where, $|X\rangle_C$ is a fixed (normalized) state of system \mathcal{H}_C , $|0\rangle_B$ is a blank ancilla state which is transformed to a clone of $|e_i\rangle_A$, and $\{|X_i\rangle_C\}$ are the fixed orthonormal basis vectors of cloning machine. The state is symmetric in the first two systems. The real coefficients p and q must satisfy the following relation in order to ensure unitarity of the QCM transformation:

$$p^2 + 2(d-1)q^2 = 1. \quad (28)$$

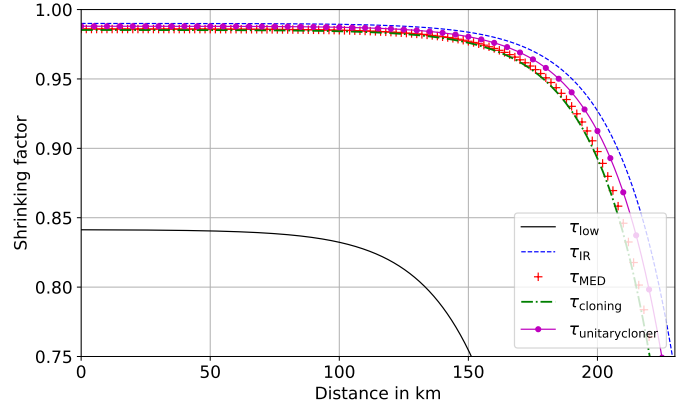


FIG. 6: Shrinking factor corresponding to the lower bound (τ_{low}), IR attack (τ_{IR}), MED attack (τ_{MED}), optimal cloning (τ_{cloning}) and unitary cloning ($\tau_{\text{unitarycloner}}$) attacks at different channel lengths. A channel loss of 0.2dB/Km and a detector efficiency of 10% is used in Eq. 6 to find the bit error rate.

We use the analytical solution given in Appendix B of [43] to find the best cloning fidelity for the 3-pulse DPS states. Based on the analytical solution given in [43], we find that the optimal q in eq. (27) is 0.23. The average fidelity of the cloned copies is found to be 0.78.

We now use the same approach as in the case of the optimal cloning attack discussed in Sec. IV to estimate the bit error rate due to the unitary cloning attack. As discussed in Appendix B, the BER in the case if the unitary cloner evaluates to 0.15. Thus the fraction of bits that can be intercepted by the eavesdropper to perform the unitary cloning attack is $6.66e_b$. After cloning, Eve is allowed to do a minimum error discrimination of the states just as in the case of the optimal cloning attack of the previous section. On running the SDP, it is found that the success probability of correct discrimination is 0.603. Thus the key rate in the presence of this attack is

$$R_{\text{UCloning}} = -\frac{2}{3}p_{\text{click}} \left[-\left(\frac{2}{3}\right)6.66e_b \cdot \log_2 0.603 + \left(1 - \left(\frac{2}{3}\right)6.66e_b\right) + f(e_b) \cdot h(e_b) \right]. \quad (29)$$

Fig. 6 shows the shrinking factor of the DPS protocol under all the attacks discussed so far. We see that cloning based on unitary transformation is not optimal compared to the map based cloning. The fidelity of cloning is lower and hence the ability to distinguishing the cloned state by Eve is low. Moreover, none of the sophisticated attacks are close to the lower bound.

VI. Conclusion

We have quantified the secure key rate for the 3-pulse DPS QKD protocol in the presence of minimum error discrimination and cloning attacks. For both these attacks, we have identified the optimal strategy for the eavesdropper, for the specific set of signal states used in the 3-pulse DPS

TABLE III: Bit error rates introduced in various attacks. μ - mean photon number, T - transmission loss, e - error rate due to implementation. The probability of success is the probability of the right identification of a state. I & R refer to intercept and resend attack

Protocol	General I & R	I & R - USD/MED	Cloning attack
Pulse train DPS[17] (WCS)	QBER = 0.25, 2e fraction with Eve [21]	USD prob. of success = $1 - e^{-2\mu}$	-
3-pulse DPS (Single photon)	QBER = 0.33 e fraction with Eve [18]	MED prob. of success = 0.75	prob. of success = 0.78, QBER = 0.13
3-pulse DPS (WCS)	QBER= 0.33, $\frac{2}{9}e^{-\mu}\mu$ fraction with Eve	USD prob. of success = $1 - e^{-2\mu}$	-
n-pulse DPS	Learning rate = $\frac{n-1}{n^2}$ [24]	MED $n = 4, p_{\text{succ}} = 0.50$ $n = 5, p_{\text{succ}} = 0.31$	-

protocol. We further note that these attack strategies can be implemented by realising specific maps and are realistic in the sense that they do not require quantum memory.

Our results indicate that these sophisticated attacks are in fact comparable to the simple intercept and resend attack in terms of the information gained by the adversary. An eavesdropper gets only as much information as a simple Bob-like intercept and resend strategy even if she uses the minimum error discrimination or cloning attack described here. Furthermore, these explicit attack strategies give much higher secure key rates than the lower bound predicted using inequalities such as the Cauchy inequality. As a point of comparison, we summarize the various known individual attacks and the corresponding figures of merit in Table III.

Our work fills a certain gap that existed in the literature, with regards to individual attacks on the DPS QKD protocol. However, we have entirely focused on the ideal, single-photon DPS protocol here. Going forward, it would be interesting to see how these individual attacks fare in

the context of more realistic phase-based QKD protocols involving weak coherent sources [44].

Although unconditional security of ideal single photon DPS QKD is known under general, collective attacks, it is useful to benchmark the effectiveness of specific individual attacks so as to be able to assess their relative strengths. The fact that the secure key rates in the presence of the individual attacks studied here are still higher than the lower bound on the secure key rate also suggests that these rates are of more practical relevance. Essentially, the secure key rates under such explicit attacks give a better sense of the realistic key rates and distances for QKD protocols.

Acknowledgments

Thanks to MeitY vide sanction 13(33)/2020-CC&BT. This research was supported in part by a grant from the Mphasis F1 Foundation to the Centre for Quantum Information, Communication, and Computing (CQuICC).

-
- [1] C. H. Bennett and G. Brassard, *Theoretical Computer Science* **560**, 7 (2014).
 - [2] C. H. Bennett, F. Bessette, G. Brassard, L. Salvail, and J. Smolin, *Journal of Cryptology* **5**, 3 (1992).
 - [3] A. K. Ekert, *Phys. Rev. Lett.* **67**, 661 (1991).
 - [4] M. Curty and N. Lütkenhaus, *Phys. Rev. A* **71**, 062301 (2005).
 - [5] B. Huttner, N. Imoto, N. Gisin, and T. Mor, *Phys. Rev. A* **51**, 1863 (1995).
 - [6] N. Lütkenhaus and M. Jahma, *New Journal of Physics* **4**, 44 (2002).
 - [7] Biham, Boyer, Brassard, van de Graaf, and Mor, *Algorithmica* **34**, 372 (2002).
 - [8] V. Scarani, H. Bechmann-Pasquinucci, N. J. Cerf, M. Dušek, N. Lütkenhaus, and M. Peev, *Rev. Mod. Phys.* **81**, 1301 (2009).
 - [9] F. Xu, X. Ma, Q. Zhang, H.-K. Lo, and J.-W. Pan, *Rev. Mod. Phys.* **92**, 025002 (2020).
 - [10] P. W. Shor and J. Preskill, *Phys. Rev. Lett.* **85**, 441 (2000).
 - [11] R. Renner, *International Journal of Quantum Information* **06**, 1 (2008), <https://doi.org/10.1142/S0219749908003256>.
 - [12] C. Portmann and R. Renner, *Rev. Mod. Phys.* **94**, 025008 (2022).
 - [13] V. Scarani and R. Renner, *Phys. Rev. Lett.* **100**, 200501 (2008).
 - [14] M. Hayashi, *Phys. Rev. A* **76**, 012329 (2007).
 - [15] L. Sheridan, T. P. Le, and V. Scarani, *New Journal of Physics* **12**, 123019 (2010).
 - [16] R. Y. Q. Cai and V. Scarani, *New Journal of Physics* **11**, 045024 (2009).
 - [17] K. Inoue, E. Waks, and Y. Yamamoto, *Phys. Rev. Lett.* **89**, 037902 (2002).
 - [18] S. Ranu, G. Shaw, A. Prabhakar, and P. Mandayam, 2017 IEEE Workshop on Recent Advances in Photonics (WRAP) 10.1109/WRAP.2017.8468572 (2017).
 - [19] K. Inoue, *IEEE Journal of Selected Topics in Quantum Electronics* **21**, 109 (2015).
 - [20] G. Shaw, S. Sridharan, S. Ranu, F. Shingala, P. Mandayam, and A. Prabhakar, *IEEE Photonics Journal* **14**, 1 (2022).
 - [21] E. Diamanti, *ProQuest Dissertations and Theses*, 166 (2006).
 - [22] T. Sasaki, Y. Yamamoto, and M. Koashi, *Nature* **509**, 475 (2014).
 - [23] Y. Hatakeyama, A. Mizutani, G. Kato, N. Imoto, and K. Tamaki, *Phys. Rev. A* **95**, 042301 (2017).
 - [24] S. K. Ranu, A. Prabhakar, and P. Mandayam, *Quantum Information Processing* **20**, 67 (2021).
 - [25] E. Waks, H. Takesue, and Y. Yamamoto, *Phys. Rev. A* **73**,

- 012344 (2006).
- [26] K. Wen, K. Tamaki, and Y. Yamamoto, Phys. Rev. Lett. **103**, 170503 (2009).
- [27] C. Branciard, N. Gisin, and V. Scarani, New Journal of Physics **10**, 013031 (2008).
- [28] A. Mizutani, Y. Takeuchi, and K. Tamaki, Phys. Rev. Res. **5**, 023132 (2023).
- [29] M. Sandfuchs, M. Haberland, V. Vilasini, and R. Wolf, Security of differential phase shift qkd from relativistic principles (2023), arXiv:2301.11340 [quant-ph].
- [30] A. Chefles, Physics Letters A **239**, 339 (1998).
- [31] C. W. Helstrom, Journal of Statistical Physics **1**, 231 (1969).
- [32] C. Branciard, N. Gisin, N. Lutkenhaus, and V. Scarani, Quantum Info. Comput. **7**, 639–664 (2007).
- [33] L. Gyongyosi and S. Imre, in *Proceedings of the 4th WSEAS International Conference on Computer Engineering and Applications*, CEA'10 (World Scientific and Engineering Academy and Society (WSEAS), Stevens Point, Wisconsin, USA, 2010) p. 121–126.
- [34] Y. Okubo, F. Buscemi, and A. Tomita, AIP Conference Proceedings **1110**, 355 (2009).
- [35] T. Durt, D. Kaszlikowski, J.-L. Chen, and L. C. Kwek, Phys. Rev. A **69**, 032313 (2004).
- [36] A. Molina, T. Vidick, and J. Watrous, in *Theory of Quantum Computation, Communication, and Cryptography*, edited by K. Iwama, Y. Kawano, and M. Muraio (Springer Berlin Heidelberg, Berlin, Heidelberg, 2013) pp. 45–64.
- [37] J. Watrous, Similarity and distance among states and channels, in *The Theory of Quantum Information* (Cambridge University Press, 2018) p. 124–200.
- [38] M. Grant and S. Boyd, CVX: Matlab software for disciplined convex programming, version 2.1, <https://cvxr.com/cvx> (2014).
- [39] M. Grant and S. Boyd, *Recent Advances in Learning and Control*, Lecture Notes in Control and Information Sciences (Springer-Verlag Limited, 2008) pp. 95–110.
- [40] W. K. Wootters and W. H. Zurek, Nature **299**, 802 (1982).
- [41] J. Watrous, *The Theory of Quantum Information*, 1st ed. (Cambridge University Press, 2018) Chap. 1.
- [42] V. Bužek and M. Hillery, Phys. Rev. Lett. **81**, 5003 (1998).
- [43] A. Mitra and P. Mandayam, Journal of Physics A: Mathematical and Theoretical **54**, 405303 (2021).
- [44] U. L. Andersen, V. Josse, and G. Leuchs, Phys. Rev. Lett. **94**, 240503 (2005).
- [45] B. Korzh, C. C. W. Lim, R. Houlmann, N. Gisin, M. J. Li, D. Nolan, B. Sanguinetti, R. Thew, and H. Zbinden, Nature Photonics **9**, 163 (2015).
- [46] D. Dieks, Physics Letters A **126**, 303 (1988).
- [47] M. Curty, L. L. Zhang, H.-K. Lo, and N. Lütkenhaus, Quantum Info. Comput. **7**, 665–688 (2007).
- [48] J. S. Sidhu, M. S. Bullock, S. Guha, and C. Lupo, Quantum **7**, 1025 (2023).
- [49] M. Lucamarini, Z. L. Yuan, J. F. Dynes, and A. J. Shields, Nature **557**, 400 (2018).

A. Choi matrix and Optimal Cloning Map

Here we describe the action of the optimal cloning attack described in Sec. IV B, on the 3-pulse DPS states. To find the final cloned state shared between the receiver (Bob) and the eavesdropper (Eve), we calculate the trace, $\text{Tr}(X\rho)$, where X is the Choi matrix obtained by solving the SDP in Eq. (12) and ρ is the density matrix corresponding to

the state to be cloned. For example, evaluating $\text{Tr}(X\rho_{+,+})$ gives us the two-qutrit state that is shared between Bob and Eve after the cloning map. Finally, to obtain the state reaching Bob, we simply trace out Eve's qutrit. On doing this we notice that the density matrix initially with Alice,

$$\rho_{+,+} = \frac{1}{3} \begin{pmatrix} 1 & 1 & 1 \\ 1 & 1 & 1 \\ 1 & 1 & 1 \end{pmatrix}, \quad (\text{A1})$$

gets transformed to,

$$\tilde{\rho}_{+,+} = \begin{pmatrix} \frac{1}{3} & 0.23 & 0.23 \\ 0.23 & \frac{1}{3} & 0.23 \\ 0.23 & 0.23 & \frac{1}{3} \end{pmatrix}. \quad (\text{A2})$$

Similarly, the action of the optimal cloning map on the other states can be evaluated as follows.

$$\rho_{+,-} = \frac{1}{3} \begin{pmatrix} 1 & 1 & -1 \\ 1 & 1 & -1 \\ -1 & -1 & 1 \end{pmatrix} \rightarrow \begin{pmatrix} \frac{1}{3} & 0.23 & -0.23 \\ 0.23 & \frac{1}{3} & -0.23 \\ -0.23 & -0.23 & \frac{1}{3} \end{pmatrix},$$

$$\rho_{-,+} = \frac{1}{3} \begin{pmatrix} 1 & -1 & 1 \\ -1 & 1 & -1 \\ 1 & -1 & 1 \end{pmatrix} \rightarrow \begin{pmatrix} \frac{1}{3} & -0.23 & 0.23 \\ -0.23 & \frac{1}{3} & -0.23 \\ 0.23 & -0.23 & \frac{1}{3} \end{pmatrix},$$

$$\rho_{-,-} = \frac{1}{3} \begin{pmatrix} 1 & -1 & -1 \\ -1 & 1 & 1 \\ -1 & 1 & 1 \end{pmatrix} \rightarrow \begin{pmatrix} \frac{1}{3} & -0.23 & -0.23 \\ -0.23 & \frac{1}{3} & 0.23 \\ -0.23 & 0.23 & \frac{1}{3} \end{pmatrix}.$$

Thus we see that the effect of the optimal cloning map on the 3-pulse DPS states is similar to the depolarizing channel of the form

$$\text{Tr}_{\text{Eve}}[\Phi(\rho)] \rightarrow (1-p)\rho + \frac{p}{d}I, \quad (\text{A3})$$

with $d = 3$ and $p = 0.31$. In other words, the set of states received by Bob after the optimal cloning attack can be written as,

$$\tilde{\rho}_{\pm,\pm} = \text{Tr}_{\text{Eve}} \Phi(\rho_{\pm,\pm}) \rightarrow (1-0.31)\rho_{\pm,\pm} + \frac{0.31}{3}I. \quad (\text{A4})$$

B. Effect of the Unitary cloner

We describe the optimal unitary cloner and the best fidelity of cloning obtained for the 3-pulse DPS states, following [43]. Recall that the general symmetric cloning transformation described in Eq. 27

$$\begin{aligned} |e_i\rangle_A |0\rangle_B |X\rangle_C &\rightarrow p|e_i\rangle_A |e_i\rangle_B |X_i\rangle_C \\ &+ q \sum_{j \neq i} (|e_i\rangle_A |e_j\rangle_B + |e_j\rangle_A |e_i\rangle_B) |X_j\rangle_C, \end{aligned} \quad (\text{B1})$$

is unitary when the parameters p and q satisfy $p^2 + 2(d-1)q^2 = 1$. For any ensemble of states, an analytical solution for the optimal values of q and p was derived in [43]. In our case, the ensemble of states in consideration is the set of DPS states $|\psi\rangle_{\pm,\pm}$. Finding the best fidelity requires us to expand the ensemble in a basis such that the fourth power of the coefficients in the state expansion are maximized. This happens when the basis set is the eigenbasis for at least one of the states in the input ensemble. To this end, we consider the basis, already used in estimating the error rate for the optimal cloner in Sec. IV B.

$$\begin{aligned} |e_1\rangle &= \frac{1}{\sqrt{3}} [|1\rangle + |2\rangle + |3\rangle] \\ |e_2\rangle &= \frac{1}{\sqrt{6}} [|1\rangle + |2\rangle - 2|3\rangle] \\ |e_3\rangle &= \frac{1}{\sqrt{2}} [|1\rangle - |2\rangle]. \end{aligned}$$

The DPS states can then be expanded in this basis as follows.

$$\begin{aligned} |\psi\rangle_{+,+} &= \frac{1}{\sqrt{3}} [|1\rangle + |2\rangle + |3\rangle] = |e_1\rangle \\ |\psi\rangle_{+,-} &= \frac{1}{\sqrt{3}} [|1\rangle + |2\rangle - |3\rangle] = \frac{1}{3}|e_1\rangle + \frac{2\sqrt{2}}{3}|e_2\rangle \\ |\psi\rangle_{-,+} &= \frac{1}{\sqrt{3}} [|1\rangle - |2\rangle + |3\rangle] \\ &= \frac{1}{3}|e_1\rangle - \frac{\sqrt{2}}{3}|e_2\rangle + \frac{\sqrt{2}}{\sqrt{3}}|e_3\rangle \\ |\psi\rangle_{-,-} &= \frac{1}{\sqrt{3}} [|1\rangle - |2\rangle - |3\rangle] \\ &= -\frac{1}{3}|e_1\rangle + \frac{\sqrt{2}}{3}|e_2\rangle + \frac{\sqrt{2}}{\sqrt{3}}|e_3\rangle. \end{aligned}$$

We find the optimal q value using the ensemble of DPS states expanded in this basis, resulting in $q_{\text{opt}} = 0.23$. In the qutrit basis $\{|1\rangle, |2\rangle, |3\rangle\}$, the transformation of the DPS states can be expressed as below.

$$\rho_{+,+} = \frac{1}{3} \begin{pmatrix} 1 & 1 & 1 \\ 1 & 1 & 1 \\ 1 & 1 & 1 \end{pmatrix} \rightarrow \begin{pmatrix} \frac{1}{3} & 0.28 & 0.28 \\ 0.28 & \frac{1}{3} & 0.28 \\ 0.28 & 0.28 & \frac{1}{3} \end{pmatrix},$$

$$\rho_{+,-} = \frac{1}{3} \begin{pmatrix} 1 & 1 & -1 \\ 1 & 1 & -1 \\ -1 & -1 & 1 \end{pmatrix} \rightarrow \begin{pmatrix} 0.28 & 0.22 & -0.25 \\ 0.22 & 0.28 & -0.25 \\ -0.25 & -0.25 & 0.44 \end{pmatrix},$$

$$\rho_{-,+} = \frac{1}{3} \begin{pmatrix} 1 & -1 & 1 \\ -1 & 1 & -1 \\ 1 & -1 & 1 \end{pmatrix} \rightarrow \begin{pmatrix} 0.36 & -0.25 & 0.14 \\ -0.25 & 0.36 & -0.17 \\ 0.14 & -0.17 & 0.28 \end{pmatrix},$$

$$\rho_{-,-} = \frac{1}{3} \begin{pmatrix} 1 & -1 & -1 \\ -1 & 1 & 1 \\ -1 & 1 & 1 \end{pmatrix} \rightarrow \begin{pmatrix} 0.36 & -0.25 & -0.17 \\ -0.25 & 0.36 & 0.14 \\ -0.17 & 0.14 & 0.28 \end{pmatrix}.$$

Similar to the analysis done in Sec. IV B, we find the error rate at Bob due to the action of the unitary cloner. $\rho_{+,+}$ after unitary cloning remains to be diagonal in the basis given above and we determine the action of the MZI on the basis and thus the state to find the probability of the erroneous click. For the rest of the states we do a spectral decomposition and find the action of MZI on the eigenbasis, which then can be used to find the error rate of the cloned states.

C. Finite size effects

Finite size effects has been widely studied for QKD protocols and is said to be the limiting factor in many cases. Here we include the finite size effects to the secure key rate against individual attacks. The three parameters that needs to be considered are

1. The statistical fluctuations in parameter estimation (PE) (fluctuations in QBER),
2. Failure probability of error correction procedure,
3. Failure probability of privacy amplification (PA) protocol used.

The first one is dominant and is orders larger than the other two. Since the failure probability of the EC and PA procedures scale as the collision probability of the hash functions used. Therefore they are usually of the order of 10^{-12} . To account for the finite size correction in the qubit error rate statistics, we use the tail bound derived in [45]. If e_{obs} denotes the observed QBER and e_{key} is the actual QBER of the key sifted, the bound is given as [45],

$$e_{\text{key}} \leq e_{\text{obs}} + t, \quad (\text{C1})$$

where

$$\begin{aligned} t(n, k, e, \epsilon') &:= \sqrt{\frac{2(n+k)e(1-e)}{kn} \log \frac{\sqrt{n+k}C(n, k, e)}{\sqrt{2\pi nke(1-e)}\epsilon'}} \\ C(n, k, e) &:= \\ &\exp\left(\frac{1}{8(n+k)} + \frac{1}{12k} - \frac{1}{12ke+1} - \frac{1}{12k(1-e)+1}\right). \end{aligned}$$

Here $n+k$ is the total number of bits sifted and k is the bits used for parameter estimation.

The deviation t is negligible for higher block lengths and we see visible effects for smaller block lengths. We plot in Fig.7 the effects for a block length of $n = 10^6$, a sample of $k = 10^4$ for parameter estimation and for confidence parameter $\epsilon' = 10^{-9}$.

D. Three-pulse DPS with a weak coherent source

The 3-pulse DPS protocol with a weak coherent source, in place of single photon sources, is not a superposition state but rather a product state and is given as:

$$|\psi\rangle_{\pm,\pm} = |\alpha\rangle_k \otimes |\pm\alpha\rangle_{k+1} \otimes |\pm\alpha\rangle_{k+2}.$$

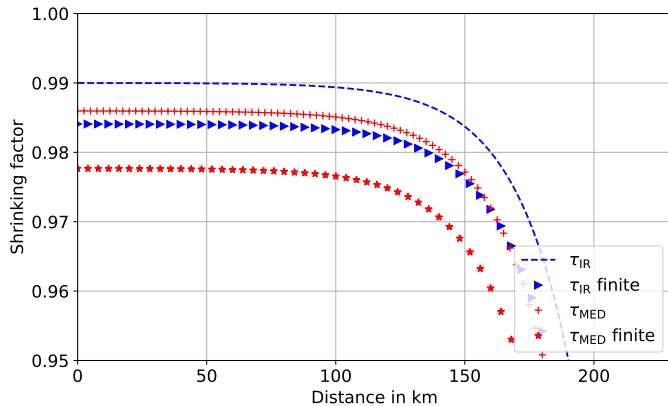


FIG. 7: Shrinking factor corresponding to IR (τ_{IR}) and MED (τ_{MED}) attacks at different channel lengths. The effect of finite size can be seen in the reduction of the key rate. A similar effect is seen for the other attacks. A channel loss of 0.2dB/Km and a detector efficiency of 10% is used in Eq. 6 to find the bit error rate.

This protocol then looks like the pulse train DPS but with two bits of data encoded in the phase between three pulses. The USD attack is then an individual attack on the 3-pulse sequences carrying two bits of data. We assume that the eavesdropper has a local oscillator phase locked to Alice's source. Thus Eve can intercept each pulse and do unambiguous state discrimination to identify whether each pulse is $|\alpha\rangle$ or $|\alpha\rangle$. The probability of successful discrimination is then given by the Ivanovic-Dieks-Peres (IDP) limit [46],

$$P_{\text{succ}} = 1 - |\langle \alpha | -\alpha \rangle| = 1 - e^{-2\mu\alpha}. \quad (\text{D1})$$

where $\mu\alpha = |\alpha|^2$. This puts a tighter upper bound on the secret key rate. At a higher mean photon number, the USD attack has more probability for right identification. Since the protocol with coherent state becomes equivalent to a pulse train DPS, the strength of the USD attack is equivalent to the one in [47] with a block size (M in [47]) of three. With the block size three, the sequential attack [47] in the 3-pulse DPS becomes an individual attack. Practical implementations of USD are now becoming more possible with currently available tools [48].

1. Phase randomized three-pulse DPS with weak coherent source

In this section, we look at the effectiveness of introducing a random phase at both Alice and Bob's side as a measure to protect against cloning and USD attack. When the phase is randomized, one cannot carry out the above-mentioned attacks. Since the set of states to be discriminated or cloned has increased from just $\{|\alpha\rangle, |-\alpha\rangle\}$ to states with random phases. The random phases are applied as follows:

1. Alice introduces the same random phase ϕ_a in both her delay lines.
2. Bob introduces a random phase ϕ_b in the delay line

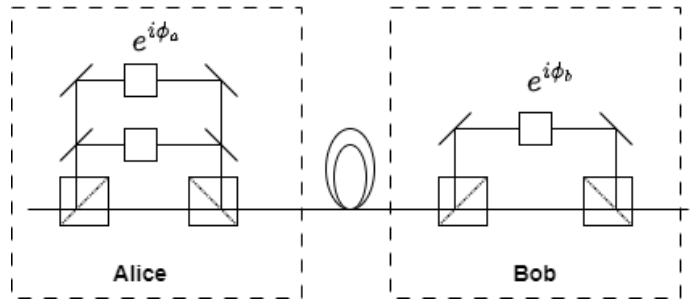


FIG. 8: 3-pulse DPS with phase randomization. Alice applies a random phase ϕ_a in both her delay lines and Bob applies a phase ϕ_b at the delay line of the asymmetric MZI.

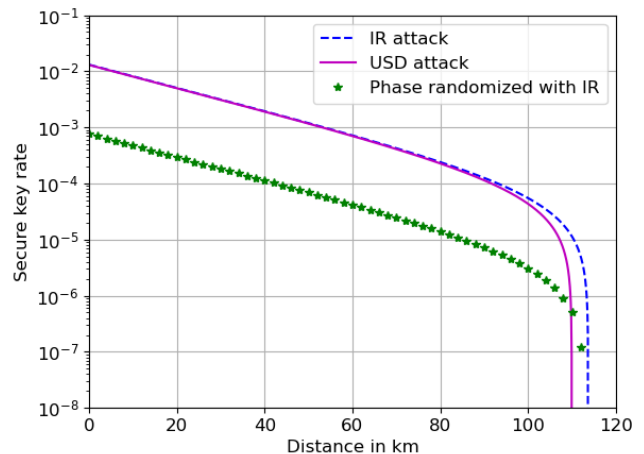


FIG. 9: Secure key rate vs distance for weak coherent state based DPS protocol in the presence of IR attack, USD attack and for protocol with phase randomization in the presence of IR attack.

of the MZI as shown in Fig. 8 in the first pulse of the three pulses sent by Alice.

When the phases introduced by Alice and Bob do not match, it increases the probability of wrong detection and thus to QBER. Following [49], we look at the error introduced when both Alice and Bob choose a random phase that is δ angle apart.

Consider the case when Alice sends the state $\{|e^{i\phi_a}\alpha\rangle_{k+2} \otimes |e^{i\phi_a}\alpha\rangle_{k+1} \otimes |\alpha\rangle_k\}$. In the absence of any random phase, the output should ideally be a click in the constructive port at time instants 2 and 3. In the presence of a random phase by Alice and Bob, it can be calculated using the input-output relation shown in Fig.10, that the state reaching the destructive port for the second time instant is

$$|ie^{i\phi_a}(1 - e^{i\delta})\rangle,$$

where $\delta = \phi_b - \phi_a$. The probability of detection in the destructive port is the QBER and is given as

$$\text{QBER} = 1 - e^{-\alpha^2 \sin^2 \delta/2} \approx \alpha^2 \sin^2 \delta/2. \quad (\text{D2})$$

Thus, the QBER introduced due to phase randomization depends on the mean photon number (α) and the phase difference (δ) between the random phases. Higher the phase difference, higher the QBER. Hence we look at a post-selection method in which Alice and Bob announce and choose only phases that lie within a small range. Say the interval $[0, 2\pi]$ is cut into M slices. The pulses in which both Alice and Bob select random phases within the same slice is only used for the secret key. We find the average QBER when δ lies within a slice and find that the QBER approaches zero as M is greater than 15. We use 16 slices and hence the maximum variation between the random phase or δ is $\pi/8$. We now use this to calculate the QBER and plot the secret key rate for a mean photon number of 0.4.

From Fig 9, It should be noted that the curve with phase randomization is lower than the curve with USD attack

since there is a further sifting factor of $1/16$ multiplied for Alice and Bob to choose the same phase slice. If we ignore the sifting factor, phase randomization provides a marginal increase in distance at high mean photon numbers.

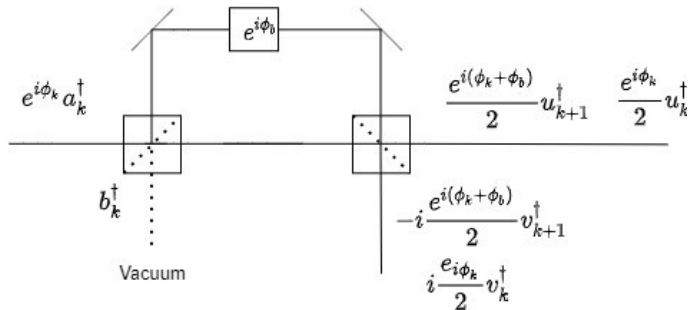


FIG. 10: Input-output relation for asymmetric MZI with phase.